Available online at www.sciencedirect.com
SCIENCE DIRECT®
ELSEVIER
Journal of Nuclear Materials 320 (2003) 265–271
journal of nuclear materials
www.elsevier.com/locate/jnucmat

Hydrogen absorption by Pd-coated ZrNi prepared by using Barrel-Sputtering System

M. Hara [a,*], Y. Hatano [a], T. Abe [a], K. Watanabe [a], T. Naitoh [b], S. Ikeno [b], Y. Honda [c]

[a] *Hydrogen Isotope Research Centre, Toyama University, Gofuku 3190, Toyama 930-8555, Japan*
[b] *Faculty of Engineering, Toyama University, Gofuku 3190, Toyama 930-8555, Japan*
[c] *Youtec Company, Nishihirai 986-1, Nagareyama, Chiba 270-156, Japan*

Received 12 July 2002; accepted 5 March 2003

Abstract

To improve the durability of hydrogen storage materials against surface poisoning by impurity gases, effectiveness of Pd-coating layer prepared by using a Barrel-Sputtering System was examined for ZrNi powder. The effectiveness of Pd-coating was evaluated by activation temperature, at which Pd/ZrNi poisoned by air could be activated to absorb hydrogen. Characterization of Pd-coated ZrNi (denoted as Pd/ZrNi) by scanning electron microscopy, electron probe microanalysis and X-ray diffraction showed that a uniform Pd-coating layer was formed with the barrel-sputtering system. It was found that the poisoned Pd/ZrNi sample could be activated even at 423 K to absorb hydrogen at room temperature. This exhibits remarkable contrast to bare ZrNi, which could be only activated appreciably above 1073 K. It is concluded that the Pd-coating by barrel sputtering is quite effective to avoid the effect of surface poisoning of powdery hydrogen storage materials. However, the activation at excessively high temperature resulted in the loss of high activity to absorb hydrogen. It was concluded that this phenomenon was associated with reactions between Pd and ZrNi to form PdZr and other byproducts.

PACS: 81.65.T; 82.65.Yh; 68.35.D; 34.50.D

1. Introduction

Hydride forming metals and alloys are widely used not only for hydrogen storage and supply but also hydrogen purification, vacuum pumps, catalysts, electrodes for hydrogen battery and so on [1]. Among them, one of the most promising applications is in safe handling of a large amount of tritium in thermonuclear fusion reactors [2]. For this purpose, Zr-based alloys such as ZrCo and ZrNi are attractive because the equilibrium pressure of tritium is sufficiently low at room temperature and the temperature at which the equilibrium pressure reaches 1 atm is not too high [2–4], so that the tritium permeation through the container wall remains small. In their practical applications, however, there arise some severe problems that need to be dealt with, e.g., poisoning by impurity gases such as H_2O, O_2, CO, etc. [5–7], fine-powdering by hydride formation, hydrogen-induced disproportionation [8–11] and so on.

The poisoning by impurity gases is unavoidable because this kind of materials are much more active to carbon and oxygen than hydrogen, and then react with the impurity gases more rigorously. Reactions with the impurity gases cause to form surface contamination layers which significantly impair hydrogen absorption and desorption kinetics [5,7,12]. One solution to this

* Corresponding author. Tel.: +81-76 445 6922; fax: +81-76 445 6931.
E-mail address: hara@hrc.toyama-u.ac.jp (M. Hara).

0022-3115/03/$ - see front matter © 2003 Elsevier B.V. All rights reserved.
doi:10.1016/S0022-3115(03)00189-2

problem is to make surface protection layers against impurity gases on alloy surfaces [7,12–14]. The surface protection layers should not react with the impurity gases but active to hydrogen absorption, desorption and permeation. Palladium is an adequate element for this purpose. To examine the effectiveness of Pd-coating, ZrNi was selected as a model system because it satisfies the requirements of sufficiently low equilibrium pressures of hydrogen isotope at room temperature, moderate temperatures to release hydrogen isotopes at 1 atm [2,3] and sufficient stability against hydrogen-induced disproportionation [10].

Preliminary examinations of the effectiveness of surface protection layers have been carried out by use of Pd-coated ZrNi, where the Pd-coating was prepared over ZrNi powder by means of electroless plating method [12–14]. Although the coating improved the durability of ZrNi surface to impurity gases containing oxygen and carbon atoms, the coating layer was not uniform in thickness and appeared somewhat porous. In addition, the layer contained impurity elements such as phosphorus [15] and carbon [15,16] that arose from the solution used for the electroless plating. To improve these problems, a device named Barrel-Sputtering System was developed in the present study. The present paper describes effectivenss of Pd-coating layers prepared with this device on improving the durability of ZrNi powder against air exposure.

2. Experimental

2.1. Sample preparation

The sample compound, ZrNi, was prepared by arc-melting of Zr and Ni powders, whose purities were guaranteed as 99.8% and 99.9%, respectively. The ingot was prepared by repeating melt-solidification procedures three times and crushed mechanically to powder, which was sieved to about 500 μm. The powder obtained was annealed in vacuum at 873 K for 2 h before use.

The Pd-coating was carried out by use of the Barrel-Sputtering System. Fig. 1 shows a schematic diagram of the device. It consists of a vacuum chamber, rotatable cylinder (barrel), Pd-target, turbo-molecular pump backed with an oil-sealed rotary pump, pressure gauges and flow-controllers. The cylinder installed in the vacuum chamber is used for spreading sample powder inside. A target plate is set along the centerline of the barrel. The Pd-target was purchased from Toshima Seisakusyo. Its size and purity were $100 \times 50 \times 1$ mm^3 and 99.99%, respectively. Argon gas used for sputtering was purchased from Nihon Sanso, and its purity was 99.999%. The residual pressure of the system was routinely below 1×10^{-5} Pa. More details of the system will be reported in a separate paper.

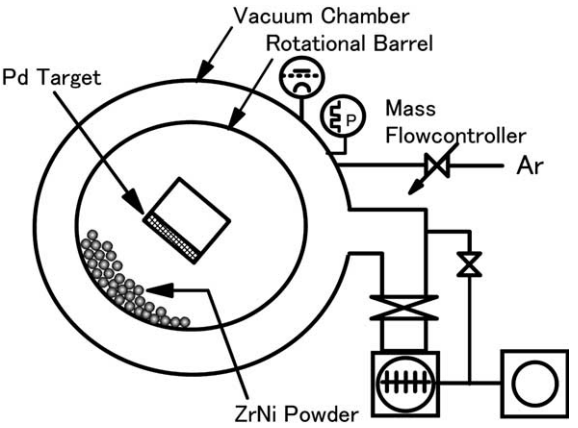

Fig. 1. Schematic diagram of the Barrel-Sputtering System.

The ZrNi powder was weighed to 2.7 g and loaded into the rotational barrel. After the chamber was evacuated below 1×10^{-4} Pa, it was separated from the vacuum pumps by the valve, and then argon gas was flowed into the chamber. The flow rate was maintained at 50 cm^3/min at 1 Pa during Pd sputtering that was carried by applying RF discharge of 13.56 MHz at 100 W. The sputtering time was fixed to 30 min, and the rotational speed of the barrel was set to 30 rpm. The Pd-target was cooled by water during sputtering, while no active temperature control of ZrNi powder as well as temperature measurement was performed in the present study.

The crystallinity of the prepared material was examined by an X-ray diffractometer of Philips PW1820 at room temperature. In addition, the surface morphology and element distributions were observed with a scanning electron microscope (Hitachi S3500H).

2.2. Durability tests

Durability of bare ZrNi and Pd/ZrNi against impurity gases was examined by ease of their activation for hydrogen absorption after surface poisoning. To contaminate the surface to a serious extent, the sample was exposed to air at room temperature for a given period of time. Then the durability to air exposure was compared by temperatures at which the sample could be activated to absorb hydrogen. A high vacuum system was used for these measurements. It consisted of a reaction vessel made of quartz glass, turbo-molecular pump with a rotary pump, vacuum gauge, quadrupole mass spectrometer and two capacitance manometers. The residual pressure was routinely below 1×10^{-5} Pa. Hydrogen gas used was purchased from Nihon Sanso. Its purity was guaranteed above 99.99995%. It was used without further purification for adsorption measurements.

The activation temperature was measured by following procedures: (1) loading the sample amounting 10 mg in the reaction vessel, (2) evacuation of the reaction vessel below 5×10^{-5} Pa, (3) sample exposure to air introduced into the vessel at 100 kPa for 10 min, (4) evacuation of the vessel below 5×10^{-5} Pa, (5) vacuum heating of the sample at a given temperature for 60 min and subsequent cooling at room temperature for 90 min, (6) loading hydrogen into the reaction vessel at room temperature, (7) measuring hydrogen absorption by the sample kept at room temperature, (8) returning to the step (3) for activation at a higher temperature. The amount of loading hydrogen was set to [H]/[ZrNi] = 0.2 in each run.

3. Results and discussion

3.1. Sample characterizations

Fig. 2 shows X-ray diffraction patterns for ZrNi and Pd/ZrNi samples, where the vertical dotted lines in the figure indicate the diffraction angles for Pd appeared in the literature [17]. The pattern of the former agreed well with JCPDS data and the latter pattern could be assigned to diffraction peaks of ZrNi [18] and Pd [17], although the intensities of diffraction peaks from Pd were considerably weaker than those from ZrNi. Surface morphology and element distributions of/on the sample were observed by scanning electron microscopy and electron probe microanalysis. SEM images of ZrNi and Pd/ZrNi are shown in Fig. 3. ZrNi particles were jagged and had many cracks because the particles were prepared by mechanical crushing. Although the shape and size were not uniform, the Pd/ZrNi sample gave a considerably intense Pd-signal for all the particles, where the intensity did not differ much from spot to spot on a particle surface and also from particle to particle. In other words, palladium was deposited rather uniformly on the particles. But the signals from Zr and Ni were still observed for this sample, suggesting that the Pd-coating layer was thin.

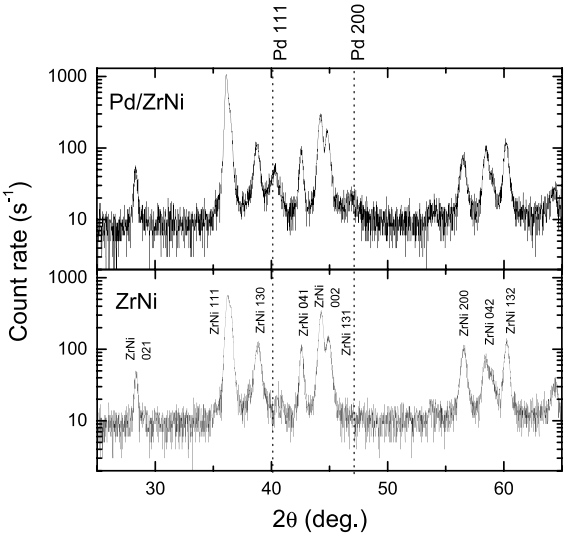

Fig. 2. X-ray diffraction patterns for Pd/ZrNi and ZrNi, Pd/ZrNi was prepared by use of barrel-sputtering system.

To estimate thickness of the Pd-coating layer, a glass plate of 18.1 cm^2 in area and 6.2886 g in weight was coated by Pd under the same conditions as Pd/ZrNi preparation and its weight gain was measured. The weight gain by the coating was 0.0248 g. By assuming that the coating layer had the same density as bulk palladium, the thickness on the glass plate was calculated to be 1.1×10^{-6} m. On the assumption that a ZrNi particle was in the form of sphere of 250×10^{-6} m in radius, the thickness of Pd layer that would be deposited on the cross-section of the sphere was calculated to be $\pi \times (250 \times 10^{-6})^2 \ (1.1 \times 10^{-6})$ m^3. By accounting that spherical particles could be rotated freely during sputter coating, the thickness of the deposition layer (x) is estimated from a relation as $(4/3)\pi\{(r+x)^3 - r^3\} = \pi \times r^2(1.1 \times 10^{-6})$, where r ($= 250 \times 10^{-6}$ m) is the radius of the spherical particle. Then the thickness of Pd layer on a hypothetical ZrNi particle was calculated to be 2.7×10^{-7} m. The amount of deposited Pd was estimated from this value to be [Pd]/[ZrNi] = 7.5×10^{-3} in atomic fraction. Practically, the ZrNi powder was not spherical, so that the surface area of ZrNi powder should be much larger. Then the thickness of Pd layer on the ZrNi powder is expected to be less than 2.7×10^{-7} m.

3.2. Durability against air exposure

Effectiveness of Pd-coating in reducing surface poisoning by impurity gases was evaluated by durability against air exposure as a model of serious contamination. Hydrogen absorption curves by ZrNi contaminated by air at room temperature are shown in Fig. 4, where the change in hydrogen pressure owing to absorption is plotted against elapsed time. It is noted that these curves were obtained by following the procedures mentioned in Section 2.2 and the temperatures in the figure represent the activation temperatures, i.e. the temperature of vacuum heating at step 5. Below 673 K, the hydrogen pressure remained almost constant for 1200 s, indicating that the activation was not enough and hydrogen could not be absorbed by ZrNi at room temperature. Above this temperature, the absorption became appreciable. Although the rate was considerably slow by the activation at 873 K, it increased with increasing temperature. The amount of hydrogen absorption was calculated from the pressure change. The

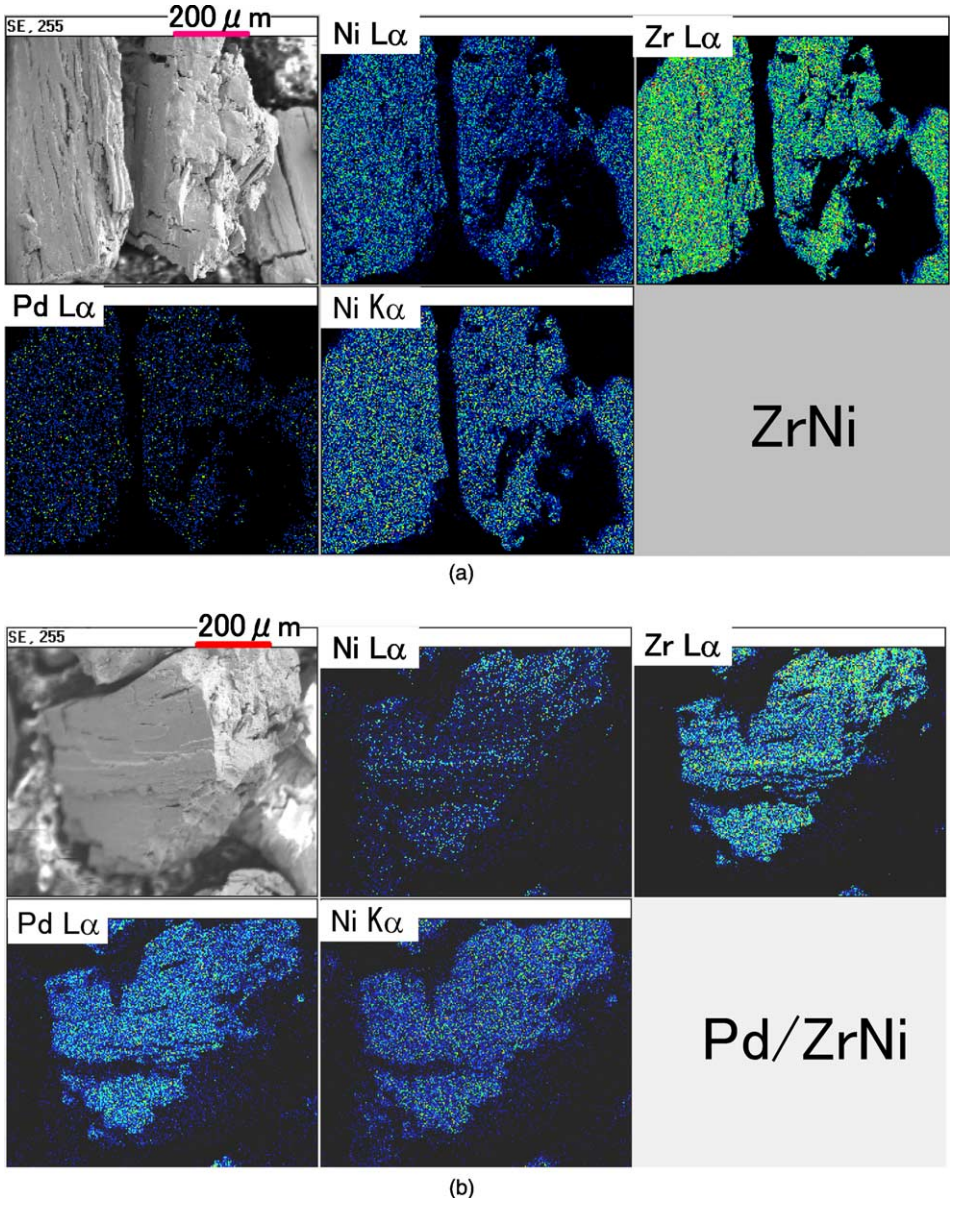

Fig. 3. Surface morphology and two dimensional element distribution images for Ni, Zr and Pd, respectively. (a) ZrNi powder and (b) Pd coated ZrNi by use of barrel-sputtering system (Pd/ZrNi).

absorption curves in Fig. 5 were obtained from Fig. 4, where the amount of hydrogen absorption is shown in a unit of atomic fraction between the number of hydrogen atoms absorbed and that of ZrNi, [H]/[ZrNi]. In this figure, it is seen that the absorption proceeded by two steps for the activation above 873 K. Initially the absorption was rather fast, but afterward the rate slowed down. Subsequently, there appeared a process of faster absorption. The first and second steps were accelerated by activation at higher temperature.

Fig. 6 shows hydrogen absorption curves for Pd/ZrNi at room temperature. It can be seen that the sample could absorb hydrogen by activation even at 423 K, exhibiting a noticeable contrast to ZrNi. By the first activation at 573 K, Pd/ZrNi showed a faster absorption rate than bare ZrNi activated at 1073 K. This enhanced absorption was reproducible as seen by the curve of the second activation. But the third activation gave even more rapid absorption. These observations indicate that Pd/ZrNi can be activated more easily than bare ZrNi

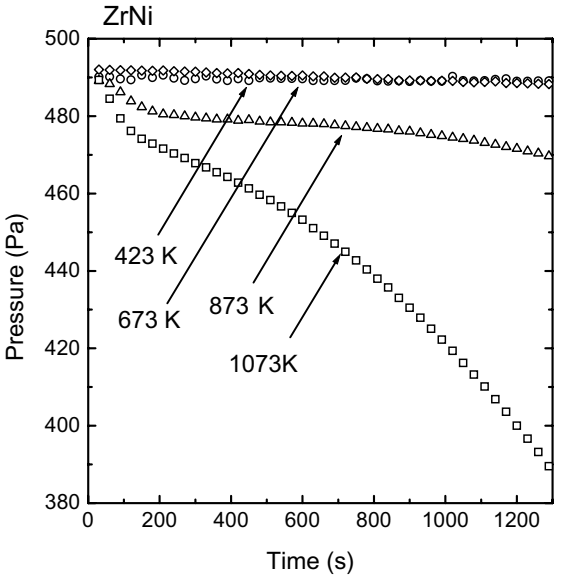

Fig. 4. Change in hydrogen pressure owing to absorption by ZrNi at room temperature. Temperatures in figure represent activation temperatures.

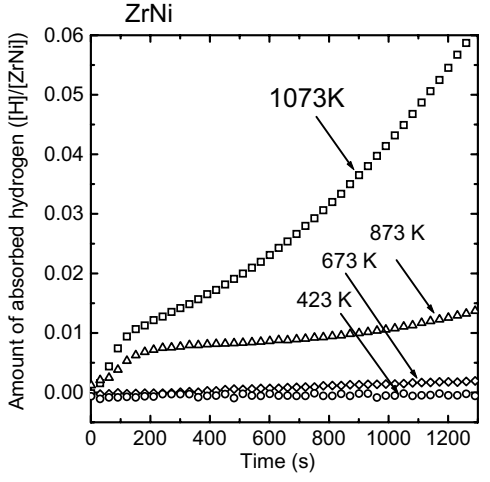

Fig. 5. Hydrogen absorption curves of ZrNi at room temperature. Temperatures in figure represent activation temperature of ZrNi.

and the Pd-coating is effective to reduce the effect of surface contamination by air exposure. But heating at higher temperatures resulted in the reverse effect as shown in Fig. 7. When the sample was activated at 673 K after the third activation at 573 K, the absorption rate decreased drastically. Once the sample lost its activation property by heating at 673 K, the high activity obtained by the activation at 573 K could not be recovered by

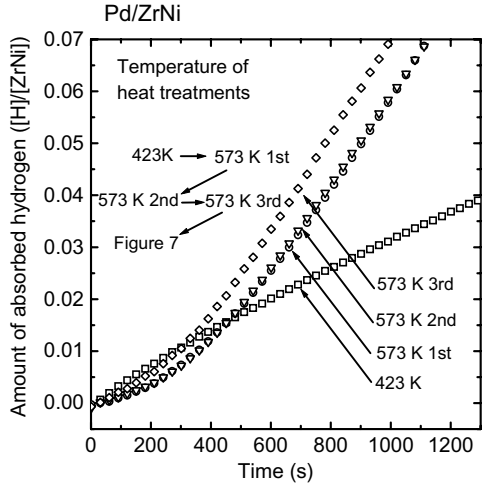

Fig. 6. Hydrogen absorption curves of Pd/ZrNi at room temperature. Activation temperatures of Pd/ZrNi were below 573 K.

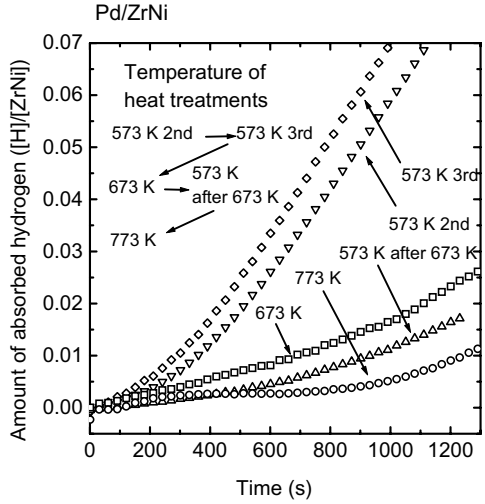

Fig. 7. Hydrogen absorption curves of Pd/ZrNi at room temperature. Activation temperature of Pd/ZrNi were up to 773 K.

repeated activation at 573 K as shown in the figure. Moreover heating at 773 K yielded even a worse absorption curve.

According to Ashida et al., electronic and crystallographic states of Pd layer on ZrNi changes significantly by vacuum heating around 973 K for 10 min [14], owing to formation of a new metallic compound of PdZr. This temperature is about 300 K higher than 673 K, at which the irreversible change in the activity behavior was observed in the present study. To examine the change in crystallographic properties of the Pd-layer, XRD

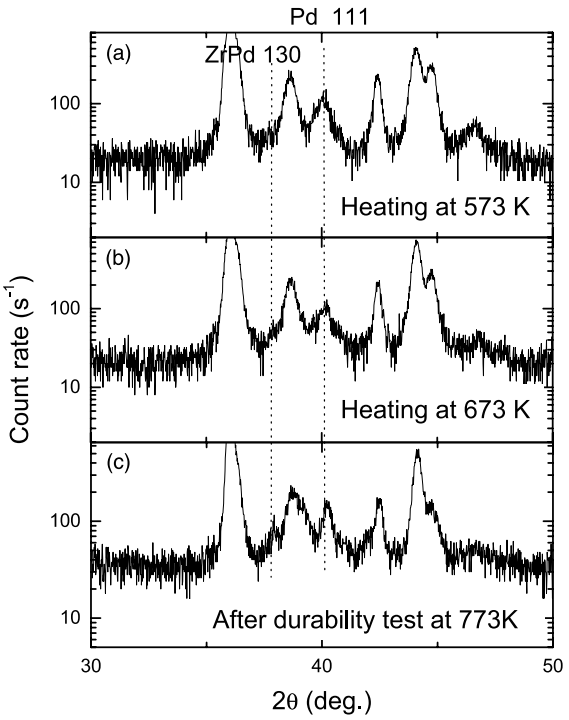

Fig. 8. X-ray diffraction patterns of Pd/ZrNi: (a) heated at 573 K in vacuum, (b) heated at 673 K in vacuum and (c) after durability test at 773 K.

patterns of Pd/ZrNi were observed for samples heated at 573, 673 and 773 K under the same conditions as activation. Fig. 8 shows the results. Although the Pd peaks were definite in all the patterns, a new peak appeared at 37.9° for the sample activated at 773 K. This peak could be assigned to PdZr(1 3 0) [19,20]. On the other hand, the pattern for the sample heated at 573 K was essentially the same as that for the as-prepared Pd/ZrNi shown in Fig. 2. As for the sample heated at 673 K, a shoulder was seen at 37.9°, corresponding to PdZr(1 3 0). These observations indicate that PdZr was formed by vacuum heating at 673 K for 60 min and much pronouncedly by heating at 773 K. Accordingly it is concluded that the irreversible change appeared by heating above 673 K is associated with the formation of PdZr on the surface of ZrNi particles. Zirconium atoms diffused to the surface can be easily oxidized or contaminated by air to deactivate the surface to hydrogen absorption and desorption [5,7,12]. The formation of PdZr suggests that other byproducts such as Pd_xZr_y, Zr_xNi_y and even Ni can be formed, although these byproducts could not be detected by XRD. Details of the reactions between the Pd-layer and ZrNi matrix are opened to further investigations.

As for the kinetics of hydrogen absorption, a characteristic feature of bare ZrNi was the two-step absorption. Although this feature appeared for the Pd/ZrNi sample activated at 423 K, the absorption by the sample activated above 573 K proceeded through one-step process. The one-step absorption curves shown in Fig. 7 could be explained by a random nucleation and crystal growth model [21–24], but the mechanism of the two-step process is not clear at present. It is interesting to note that the one-step absorption was only observed for the sample covered with crystalline Pd. Analysis of absorption curves is now ongoing and details of the analysis will be reported in a separate paper.

4. Conclusion

To improve the durability of hydrogen storage materials against surface poisoning by impurity gases, effectiveness of surface coating was studied for Pd-coated ZrNi (Pd/ZrNi) powder as a model system, where the Pd-coating was carried out by using a newly developed barrel-sputtering system. Observations of powders by scanning electron microscopy and electron probe microanalysis as well as X-ray diffraction showed that Pd was deposited rather uniformly on ZrNi particles.

The durability against impurity gases was evaluated by temperatures required for activating Pd/ZrNi and ZrNi powders exposed to air to absorb hydrogen at room temperature. It was found that ZrNi poisoned by air exposure could not be activated by vacuum heating below 423 K. For activating in appreciable extent, it requires vacuum heating around 873 K. On the other hand, Pd/ZrNi became active to absorb hydrogen by vacuum heating even at 423 K and faster hydrogen absorption took place by heating at 573 K. Further elevation of the heating temperature, however, resulted in the reduction of the absorption rate. Once this reduction occurred, Pd/ZrNi loses its ability to be activated at lower temperatures. This phenomenon was attributed to the formation of a new metallic compound, PdZr, and reduction in elemental Pd on the surface. The observations mentioned above demonstrate that the barrel-sputtering system is useful for preparing uniform coating layers to protect surface powder products from poisoning.

References

[1] G. Sandrock, S. Suda, L. Schlapbach, in: L. Schlapbach (Ed.), Topics in Applied Physics – Hydrogen in Intermetallic Compounds II, Springer-Verlag, Berlin, 1992 (Chapter 5).
[2] R.-D. Penzhorn, M. Devillers, M. Sirch, J. Nucl. Mater. 170 (1990) 217.
[3] K. Watanabe, K. Tanaka, M. Matsuyama, K. Hasegawa, Fusion Eng. Des. 18 (1991) 27.
[4] S. Konishi, T. Nagasaki, N. Yokokawa, Y. Naruse, Fusion Eng. Des. 10 (1989) 355.

[5] K. Ichimura, K. Ashida, K. Watanabe, J. Vac. Sci. Technol. A 3 (1985) 346.
[6] I. Vedel, L. Schlapbach, J. Vac. Sci. Technol. A 11 (1993) 539.
[7] K. Ashida, K. Watanabe, N. Terashita, S. Tada, S. Ikeno, Ann. Rept. Hydrogen Isotope Res. Center 14 (1994) 65.
[8] M. Devillers, M. Sirch, R.-D. Penzhorn, Chem. Mater. 4 (1992) 631.
[9] S. Konishi, T. Nagasaki, K. Okuno, J. Nucl. Mater. 223 (1995) 294.
[10] M. Hara, T. Okabe, K. Mori, K. Watanabe, Fusion Eng. Des. 49–50 (2000) 831.
[11] M. Hara, R. Hayakawa, K. Watanabe, Mater. Trans. JIM 41 (2000) 1146.
[12] K. Ashida, Y. Hatano, W. Nishida, K. Watanabe, A. Amano, K. Matsuda, S. Ikeno, J. Nucl. Sci. Technol. 38 (2001) 952.
[13] K. Ashida, K. Watanabe, S. Ikeno, K. Mori, Fusion Eng. Des. 39–40 (1998) 1049.
[14] K. Ashida, W. Nishida, J. Nagata, Y. Nishimura, K. Watanabe, Mater. Trans. JIM 40 (1999) 851.
[15] K. Ashida, K. Watanabe, S. Morozumi, K. Matsuda, S. Tada, Ann. Rept. Hydrogen Isotope Res. Center 12 (1992) 59.
[16] K. Ashida, K. Watanabe, J. Nagata, K. Mori, Ann. Rept. Hydrogen Isotope Res. Center 16 (1996) 49.
[17] JCPDS – International Center for Diffraction Data, 46-1043.
[18] JCPDS – International Center for Diffraction Data, 12-0478.
[19] JCPDS – International Center for Diffraction Data, 16-0432.
[20] L.A. Bendersky, J.K. Stalick, R. Portier, R.M. Waterstrat, J. Alloys. Comp. 236 (1996) 19.
[21] M. Avrami, J. Chem. Phys. 7 (1939) 1103.
[22] M. Avrami, J. Chem. Phys. 8 (1940) 212.
[23] M. Avrami, J. Chem. Phys. 9 (1941) 177.
[24] S.F. Hulbert, J. Br. Ceram. Soc. 6 (1969) 11.